ACS SyntheticBiology

Research Article

pubs.acs.org/synthbio

Analysis and Design of a Genetic Circuit for Dynamic Metabolic Engineering

Nikolaos Anesiadis,[†] Hideki Kobayashi,[‡] William R. Cluett,[†] and Radhakrishnan Mahadevan*[,†,§]

[†]Department of Chemical Engineering and Applied Chemistry, University of Toronto, Canada, M5S 3E5

[‡]Japan Agency for Marine Earth Science and Technology, Japan

[§]Institute of Biomaterials and Biomedical Engineering, University of Toronto, Canada, M5S 3G9

Supporting Information

ABSTRACT: Recent advances in synthetic biology have equipped us with new tools for bioprocess optimization at the genetic level. Previously, we have presented an integrated *in silico* design for the dynamic control of gene expression based on a density-sensing unit and a genetic toggle switch. In the present paper, analysis of a serine-producing *Escherichia coli* mutant shows that an instantaneous ON-OFF switch leads to a maximum theoretical productivity improvement of 29.6% compared to the mutant. To further the design, global sensitivity analysis is applied here to a mathematical model of serine production in *E. coli* coupled with a genetic circuit. The model of the quorum sensing and the toggle switch involves 13 parameters of which 3 are identified as having a significant effect on serine concentration. Simulations conducted in this reduced parameter space further identified the optimal ranges for these 3 key parameters to achieve productivity values close to the maximum theoretical values. This analysis can now be used to guide the experimental implementation of a dynamic metabolic engineering strategy and reduce the time required to design the genetic circuit components.

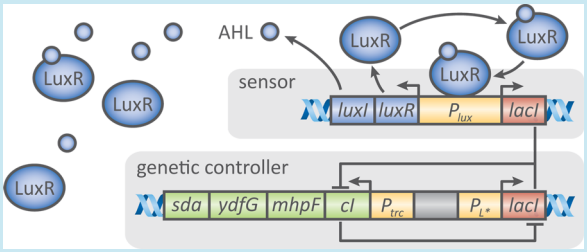

KEYWORDS: *global sensitivity analysis, quorum sensing, toggle switch, metabolic engineering*

Genetic engineering techniques have equipped metabolic engineers with a plethora of tools for gene deletion, overexpression of endogenous and expression of heterologous genes, and more recently, control of gene expression and modification of regulatory networks.[1,2] In parallel, genome-scale reconstructions of metabolic networks and constraint-based modeling have elucidated cell physiology and guided hypothesis-driven discovery in a systematic way. The systematic exploration of the feasible designs of metabolic networks would be impossible without the establishment of genome-scale modeling.[3]

Many computational strain design algorithms based on constraint-based modeling are aimed at the maximization of product yield.[4] OptKnock and OptReg were the first algorithms to identify gene deletions, overexpression and downregulation for improved product formation.[5,6] Also, a local search approach was developed to allow for more modifications than OptKnock.[7] More recently, new algorithms such as OptForce and EMILiO capable of predicting optimal flux levels for maximum production have been developed.[8,9] The objective of these strain design algorithms is to maximize product yield, which typically comes at the expense of lower growth rate and process productivity. The trade-off between yield and productivity suggests that dynamic optimization is essential.

Several dynamic optimization methods have been applied to determine the optimal control profile of fed-batch reactors.[10] These studies are limited to simple phenomenological models of bacterial growth and substrate/product inhibition. With the development of genome-scale networks, comprehensive models of metabolism have extended the understanding and predictive capability from the bioreactor to the genetic level.[11,12] Dynamic flux balance analysis (dFBA) has been used in the past to predict fed-batch operating policies in *S. cerevisiae*[13] and optimal genetic manipulations for ethanol production in *E. coli*.[14,15] Gadkar et al. showed that when gene deletions cause growth impairment, it is optimal to dynamically control gene expression instead, with a bang−bang type of control[16] (i.e., an abrupt switch between two states). The optimal ON-OFF policy deploys an initial high growth rate phase followed by a high production phase.[14] The means to implement this strategy may be found in the area of synthetic biology.

In synthetic biology, genetic constructs are engineered and coupled with the natural genetic machinery in order to reprogram the cellular processes.[17−19] Genetic devices can be thought of as the analogues of electronic parts such as sensors, switches, logic operators, and actuators that perform specific tasks at different stages of the gene expression process.[20] Genetic engineering has provided us with regulatory parts such as promoters, ribosome binding sites, riboswitches, and RNA regulators to control gene expression at the transcription[21−23]

Received: December 3, 2012
Published: March 20, 2013

and post-transcription/translation stage.[24−29] Natural quorum sensing systems have been coupled with genetic devices to perform novel cellular tasks[30−32] and reengineered to induce expression of recombinant proteins.[33] Also, properties such as specificity and sensitivity to the inputs of the quorum sensing system have been altered to create a series of LuxR variants with different responses.[34,35]

Anesiadis et al.[36] proposed a modular genetic circuit design similar to that of Kobayashi et al.[30] to couple a natural quorum sensing module and the genetic toggle switch[37] to bacterial metabolism. The objective of the integrated genetic circuit is to implement density-dependent expression of genes contributing to growth in the optimal ON-OFF fashion suggested by Gadkar et al. This process utilizes a programmable synthetic feedback loop without the need for external inducer and monitoring (see Figure 1 and Methods section for more details).

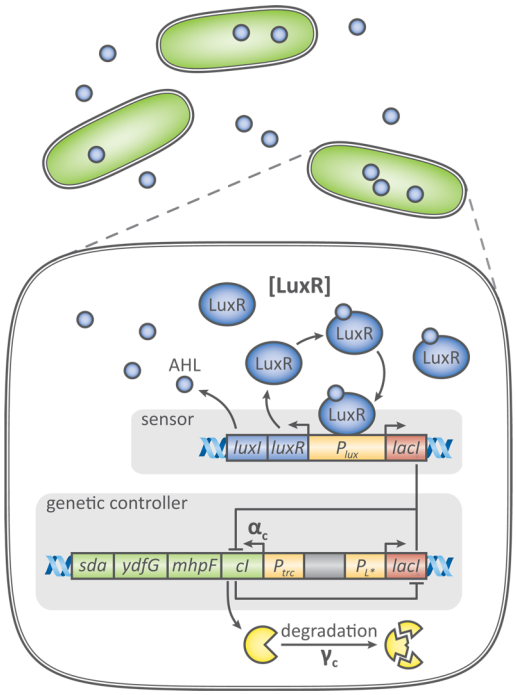

Figure 1. The genetic circuit consists of the sensor and the genetic controller plasmids (with genes *sda*, *ydfG*, and *mhpF* controlling the fluxes of ACALD and LSERDHr in the toggle switch). The most significant parameters as identified by the global sensitivity analysis are highlighted in bold (α_C, γ_C, and LuxR concentration).

Mathematical modeling can play a significant role in the design and engineering of synthetic biology elements. The complexity emerging from the hierarchical structure of biochemical networks, the connectivity and interactions between the components, and the nonlinear and stochastic nature of biochemical processes all can be elucidated to a certain degree with mathematical models.[38−42] Computational models can provide us with *in silico* experiments to explore different behaviors over a range of conditions and identify correlations between the parameters. Notwithstanding, model uncertainty is an inherent attribute of mathematical models and therefore analyzing the impact of this uncertainty is crucial for the design of meaningful experiments.[43−46] Global sensitivity analysis (GSA) methods are typically applied first in the modeling building cycle presented in Kiparissides et al. to quantify the significance of the parameters on an output of the model.[47] Sensitivity analysis has provided in depth insights in the design of experiments for the optimization of genetic circuits,[48,49] RNA devices,[26] signaling pathways,[50,51] bioremediation applications,[52,53] stem cell differentiation,[54] and antibody production.[55,56]

So far, in our work we have presented the initial circuit design for an ethanol and succinate case study,[36] and we have performed a preliminary sensitivity analysis in a shorter paper.[57] The effect of the genetic circuit parameters on the important process variables such as productivity, yield, and batch time, along with determining a recommended operating range for the key design parameters, has not been explored yet and is the focus of this paper.

We begin here by developing a dFBA model of a serine-producing *E. coli* mutant predicted by the EMILiO algorithm.[9] Then, we show that by allowing the fluxes of the deleted genes to be manipulated in an ideal ON-OFF fashion, the productivity can be improved and the batch time decreased. After coupling the genetic circuit to the bacterial metabolism using nominal parameter values from the literature, global sensitivity analysis is applied to quantify the effect of circuit parameters on serine concentration. On the basis of the GSA results, we then investigate how the most important parameters impact bioprocess objectives (such as productivity, yield, and titer), batch time, and switching time of the toggle. This analysis allows us to identify the parameter space that satisfies targets, along with gaining a better understanding of the bistability and the switching time of the integrated circuit. We believe that this work now sets the stage for the experimental implementation of this metabolic engineering strategy.

RESULTS AND DISCUSSION

Strain Design and Static Strategy. First, we designed a serine-producing *E. coli* strain using the EMILiO algorithm.[9] The EMILiO algorithm was used with a minimum growth rate constraint of 0.4/h. The strain design involves a total of 10 modifications: three gene deletions and seven fine-tuned fluxes. The gene deletions include the reactions of acetaldehyde dehydrogenase (ACALD), L-serine dehydrogenase (LSERDHr), and L-serine deaminase (SERDL). The fine-tuned fluxes include the phosphoglycerate dehydrogenase (PGCD), phosphotransacetylase (PTAr), acetyl-CoA synthetase (ACS), methylenetetrahydrofolate (MTHFD), pyruvate dehydrogenase (PDH), pyruvate formate lyase (PFL), and tryptophanase (TRPAS2). The values of the fine-tuned fluxes are given in the Supporting Information.

The production envelope of the modifications mentioned above is shown in Figure 2. The growth rate and serine flux obtained for the baseline strain with fine-tuned fluxes (A) and the mutant (B) is shown in Table 1. The higher serine production is associated with lower growth rate (i.e., 0.4 compared to 0.75/h). This makes the dynamic control of gene expression a favorable method for optimizing productivity.

As a baseline for our comparison we use the static strategy, which is essentially the mutant strain grown in a batch reactor. The mutant strain is expected to have the longest batch time, since the maximum growth rate is 0.4/h. The batch is simulated using the dynamic flux balance formulation (dFBA) with 20 mM of initial glucose, the three genes knocked out, and the seven fluxes fixed at their optimal values. The dynamic profile of the static strategy (Supplementary Figure SI.1) results in a serine titer of 26.1 mM and batch time of 11.2 h. On the basis of these values, we can estimate the values for the three

dx.doi.org/10.1021/sb300129j | *ACS Synth. Biol.* 2013, 2, 442−452

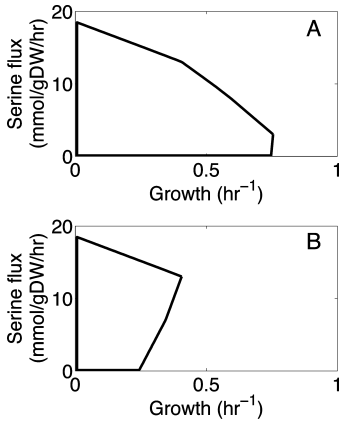

Figure 2. Production envelope of *E. coli* strain design predicted by EMILiO. The baseline strain includes 7 fine-tuned fluxes (A). The serine-producing strain includes 3 knockouts and 7 fine-tuned fluxes (B).

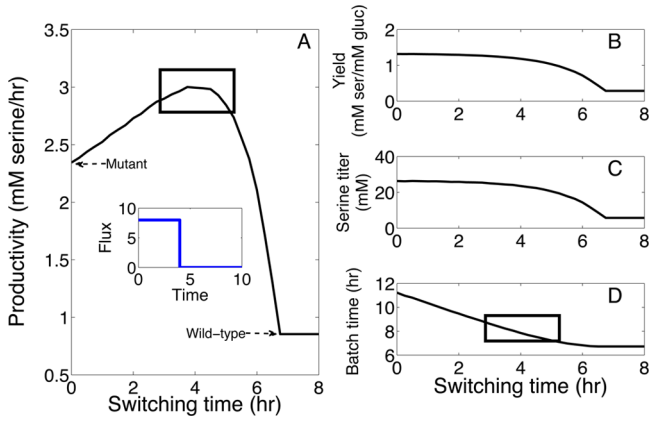

Figure 3. Productivity (A), yield (B), serine titer (C), and batch time (D) as a function of the switching time. The maximum theoretical productivity is approximately 29.6% higher than the static strategy (i.e., switching time = 0). The inset in panel A refers to a flux profile corresponding to a switching time of 4 h.

Table 1. Growth Rate and Serine Flux under Aerobic Conditions for Glucose Uptake Rate of 10 mmol/gDW/h from Flux Balance Analysis

	growth rate (h^{-1})	serine flux (mmol/gDW/h)
7 fixed fluxes	0.75	2.7
3 knockouts + 7 fixed fluxes	0.4	12.9

objectives: productivity, yield, and titer in Table 2, where we compare them with the dynamic strategy in the following section.

Table 2. Comparison of Objective Function Values for Static, Ideal Dynamic, and Dynamic Strategies[a]

	static strategy	ideal dynamic strategy	dynamic strategy
productivity (mM serine/h)	2.33	**3.02**	2.99
yield (mM serine/mM glucose)	**1.30**	1.21	1.14
serine titer (mM)	26.1	24.2	22.7
batch time (h)	11.2	8.1	7.8

[a]The dynamic strategy is based on the nominal parameter values of the genetic circuit. The maximum values of productivity and yield are in bold.

Ideal Dynamic Strategy. In the ideal dynamic strategy, we assume that the fluxes of the genes being knocked out have the same values as the wild-type initially and then go to zero when turned off (inset in Figure 3A). The fine-tuned fluxes remain at their optimal level. The ideal dynamic strategy refers to the perfect ON-OFF control, since we assume that the fluxes go to zero instantaneously. In practice, this is not realistic because (i) gene repression is a process that happens on the order of minutes to hours and (ii) even after the gene is repressed, the proteins present will catalyze the reaction before they degrade. However, the instantaneous ON-OFF control serves as a basis of comparison for the dynamic strategy. The dynamics of this switch are very important for the optimization of the process and will be studied in the following section.

Here, we define the switching time (t_S) as the time at which the switch from the ON to the OFF state occurs (the switching time should not be confused with the duration or the dynamics of the switch). In the ideal dynamic strategy, we consider the switching time to be the manipulated independent (input) variable. Serine concentration and batch time are the dependent (output) variables since they are a function of the switching time. These outputs in turn define the values of the three bioprocess objectives, namely, productivity, yield, and titer shown in Figure 3A, B, and C, respectively. Here, notice that for the two extreme values of the switching time t_S, we have the batch equivalent to the mutant if $t_S = 0$ and batch equivalent to the wild-type if t_S is greater than 6.5 h (Figure 3A). Also, the greater the switching time, the more biomass and less serine is generated (all lines in Figure 3 flatten out after 6.5 h, indicating that if the switch does not occur within the first 6.5 h, the glucose is consumed within 6.5 h and the batch time is 6.5 h). Therefore, the yield and titer of the dynamic strategy is always lower than the static strategy, i.e., the mutant or $t_S = 0$ (Figure 3B and C). However, the trade-off between biomass and product leads to a maximum productivity of 3.02 mM serine/h, which is 29.6% higher than the static strategy (2.33 mM serine/h). The increase in productivity comes as a result of the decrease in the batch time, since we generate biomass at a faster rate initially. The maximum in productivity and the associated batch time in the optimum productivity region are emphasized in the boxed areas. Note that if we want to keep the yield and titer high, we should apply a switching time that is below the optimal value (approximately 4 h), because if we apply a switching time less than 4 h, we can still improve the productivity, while keeping yield and titer high.

Dynamic Strategy. In the dynamic strategy, the genetic circuit (eqs 7−10 in the Methods section) determines the switching time. The manipulated genes and *cI* are in the ON state, resulting in high growth rate and consequently production and accumulation of AHL. When the concentration of AHL reaches a critical threshold the LuxR-AHL dimer formed initiates transcription of gene *lacI*. The production of the protein repressor from *lacI* leads to the repression of the manipulated genes and *cI*. In this section, we apply the dynamic strategy with the nominal literature values of the genetic circuit (Supplementary Figure SI.2).

The three gene deletions of the initial strain design are candidates for the dynamic gene expression. Out of the three deletions only ACALD and LSERDHr have a significant impact on growth and are therefore placed under the control of the

dx.doi.org/10.1021/sb300129j | *ACS Synth. Biol.* 2013, 2, 442−452

genetic circuit (genes *sda*, *ydfG*, and *mhpF* shown in Figure 1). The flux of SERDL has little impact on growth and therefore the gene associated is deleted.

As seen in Supplementary Figure SI.2, ACALD and LSERDHr fluxes start decreasing after approximately 4 h and are turned off completely after approximately 1 h. Similarly, Gardner et al. showed that turning off gene expression in the toggle switch is completed within less than 1 h.[37] The growth rate drops from 0.75 to 0.4/h, and glucose is fully consumed in 7.8 h (in comparison, it took 11.2 h with the static strategy). The objective values of the dynamic strategy for the nominal genetic circuit parameter values and the optimal ideal ON-OFF control are shown in Table 2.

Even without any optimization of the parameters associated with the genetic circuit, we notice a significant increase in the productivity of approximately 28.3% (2.99 vs 2.33 mM serine/h). This suggests that the initial implementation of the dynamic strategy comes very close to the maximum theoretical performance. Notice that the increase in productivity comes at the expense of lower yield and titer compared to the static strategy.

Global sensitivity analysis is applied in the next section to determine which parameters of the genetic circuit have the greatest impact on the performance of the dynamic strategy, i.e., serine productivity.

Global Sensitivity Analysis. The dynamic strategy simulated in the previous section contains many parameters associated with the quorum sensing and the toggle switch that enter the model in a highly nonlinear, interacting way. With fast simulations of dFBA problems, we can perform *in silico* experiments to study the effect of these parameters on the outputs of interest. Here, we use global sensitivity analysis to study the effect of these parameters on the initial flux levels, the switching time, the duration of the switch, and in turn the bioengineering objectives. The switching time, t_S, associated with the dynamic strategy is defined here as the time at which the manipulated fluxes reach 5% of their initial values and is seen to be approximately 5 h in Supplementary Figure SI.2C.

In Figure 4, we show the total, interaction, and individual sensitivity indices of the most significant parameters of the genetic circuit with respect to serine concentration over time. Out of 13 parameters, only 3 were found to have an average total sensitivity index higher than 0.1, namely, the toggle switch parameters γ_C and α_C and the quorum sensing parameter LuxR (average total sensitivity indices of approximately 0.54, 0.35, and 0.10, respectively). This result suggests that the process can be optimized by focusing on these three parameters, while the rest of the parameters are fixed at their nominal values.

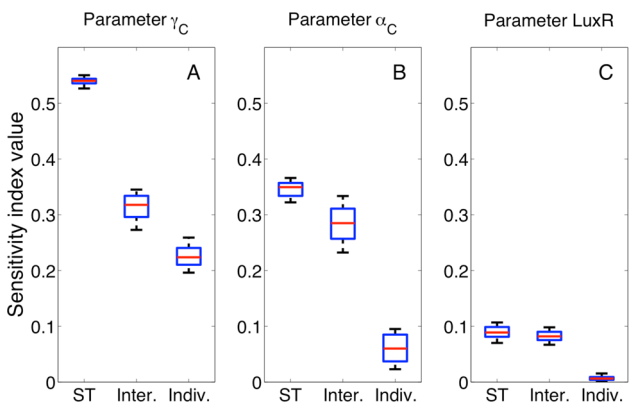

Figure 4. Sensitivity indices of parameters γ_C (A), α_C (B), and LuxR (C) for serine concentration. Total (ST), interaction (Inter.) and individual (Indiv.) indices are shown. The ranges refer to sensitivity values obtained every hour over the batch. Note that the variation of the sensitivity indices across time is not significant. The boxes show the lower quartile, the median, and the upper quartile values. The whiskers represent 1.5 times the interquartile range.

Interestingly, parameters α_L and γ_L of the genetic circuit have negligible sensitivity indices. In contrast, the toggle switch alone is a symmetric circuit, and previous analysis showed that high production and degradation rates of both genes (i.e., high α_C, α_L, γ_C, and γ_L) favor a robust and stable switch.[37] Here, analysis of the integrated circuit indicates high sensitivity of the *cI* component of the toggle (i.e., α_C and γ_C) and parameter LuxR of the quorum sensing, but insignificant sensitivity to parameters α_L and γ_L. The reason is that the integrated circuit is not symmetric and the quorum sensing induces *lacI* independently of the toggle switch.

The interaction indices are very significant for all 3 of these key parameters as they account for an average of 58%, 83%, and 93% of the total sensitivities, respectively. However, the analysis used here does not estimate the individual interactions between parameters (i.e., second, third-order effects etc.) but only the total interaction effects. Also, the global sensitivity analysis does not provide the direction of the parameter effect (e.g., whether an increase or decrease in γ_C leads to an increase or decrease in the productivity). Therefore, in order to investigate the interaction effects further, we explore the effects of changing two and three parameters at a time in the following sections.

Effect of α_C and γ_C. Figure 5A shows that the productivity of the dynamic strategy is higher than the static (flat surface shown for comparison) over a wide range of the α_C–γ_C parameter space. Productivity exhibits a maximum plateau, which broadens with increased values of α_C and γ_C. A wide plateau is desirable as it ensures robustness of the design. The value of productivity within the plateau is between 2.95 and 3 mM serine/h, which is approximately 27–29.6% higher than the static strategy (in comparison, the ideal ON-OFF controller has a maximum productivity of 3.02 mM serine/h, Table 2).

In Figure 5B and C, yield and titer are always lower than the static strategy as a consequence of the initial growth phase and tend toward the static strategy for high γ_C and low α_C values since this leads to genes being turned off and cells growing as mutants (OFF state). At this extreme, productivity also tends toward the value of the static strategy. At the other extreme, gene expression stays in the ON state throughout the batch for high α_C and low γ_C values, resulting in wild-type cells (ON state) where the objectives values are at their minima.

Figure 5D illustrates the effect of the parameters on the batch and switching time. High γ_C and low α_C values result in zero switching time (i.e., a monostable OFF state switch, since the toggle is always in the OFF state). In this region, the batch is equivalent to the mutant, and the objective values tend to the values of the static strategy. At the other extreme, high α_C and low γ_C values result in the switching time being equal to the batch time (i.e., a monostable ON state switch, since the toggle is in the ON state throughout the course of the batch). In this region, the batch is equivalent to the wild-type and the objectives values are at their minima. For values between the two extremes, there is a third region where the switching time is between 4 and 6.5 h. In this region, the toggle switches between the ON and the OFF state, resulting in what is referred to as a

dx.doi.org/10.1021/sb300129j | *ACS Synth. Biol.* 2013, 2, 442–452

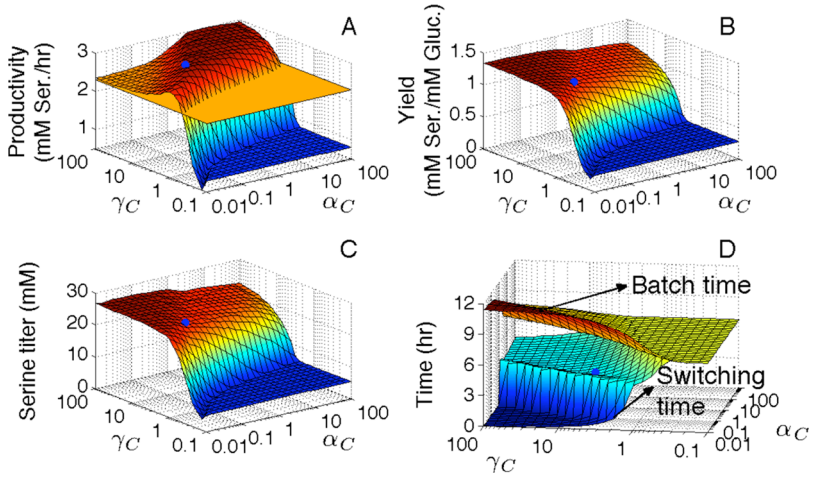

Figure 5. Effect of α_C–γ_C on productivity (A), yield (B), titer (C), and batch and switching time (D). The blue point shows the nominal values of parameters α_C and γ_C. The flat surface in panel A shows the productivity of the static strategy.

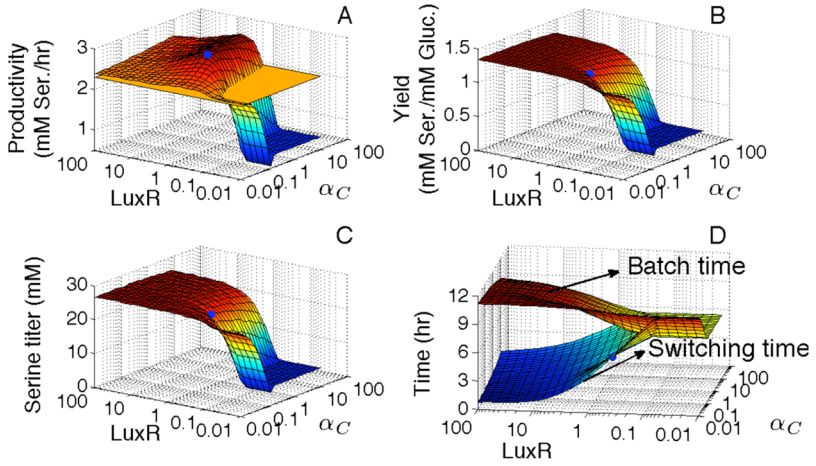

Figure 6. Effect of α_C–LuxR on productivity (A), yield (B), titer (C), and batch and switching time (D). The blue point shows the nominal values of parameters α_C and LuxR.

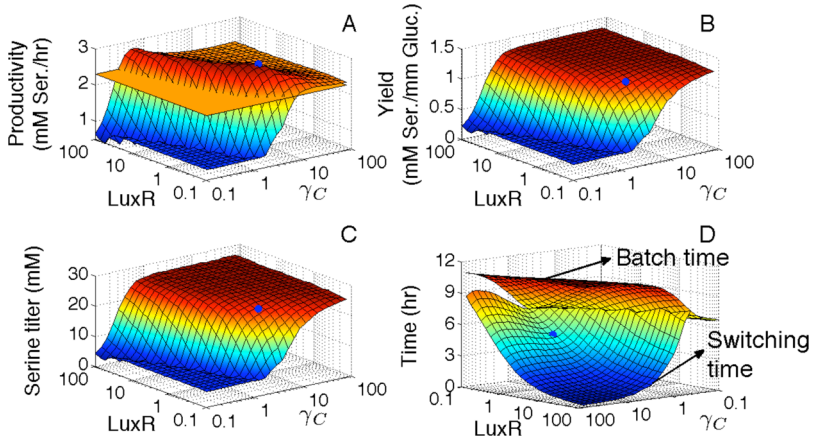

Figure 7. Effect of γ_C–LuxR on productivity (A), yield (B), titer (C), and batch and switching time (D). The blue point shows the nominal values of parameters γ_C and LuxR.

bistable switch. The area of the bistability increases with increased values of α_C and γ_C. In most of the bistable region the switching time is approximately 4 h and increases rapidly to 6.5 h when γ_C decreases, whereas α_C does not affect the switching time significantly.

To support the conditions for bistability of the toggle, Gardner[37] and Kobayashi[30] demonstrated that strong promoters (i.e., high α_C) and high degradation rates (i.e., high γ_C) increase the size of the bistable region. This result was derived based on phase-plane analysis of a mechanistic toggle switch model and was also tested in a number of plasmids with

dx.doi.org/10.1021/sb300129j | ACS Synth. Biol. 2013, 2, 442–452

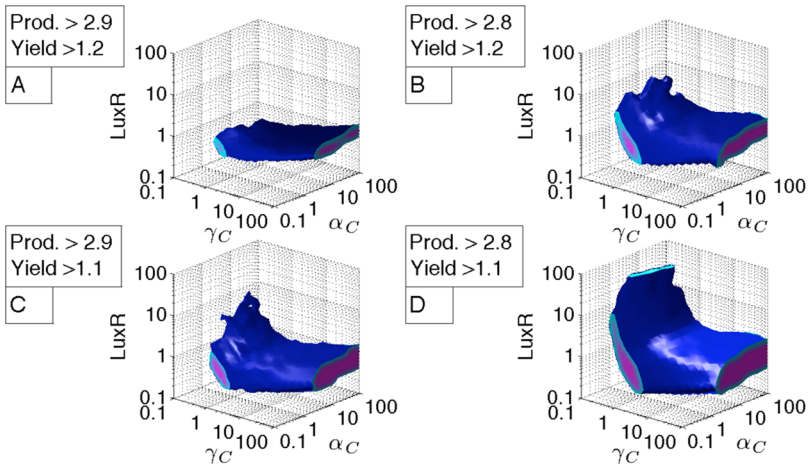

Figure 8. Effect of α_C–γ_C–LuxR on productivity and yield. Isosurfaces are shown for values of productivity higher than 2.9 and 2.8 mM serine/h and yield higher than 1.2 and 1.1 mM serine/mM glucose.

different promoter strengths. In addition, protein degradation tags were used in the plasmids to increase protein degradation rates.

Effect of α_C and LuxR. Similarly, the productivity of the dynamic strategy is higher than the static in most of the α_C–LuxR parameter space (Figure 6A). The maximum value in the plateau converges to the maximum productivity of the ideal ON-OFF controller (i.e., 3.02 mM serine/h). However, the maximum plateau when varying these two parameters is narrow (in contrast to the α_C–γ_C parameter space). The shape of the plateau suggests that fine-tuning of parameter LuxR is crucial to ensure maximum productivity.

Figure 6D reveals how parameter LuxR affects the batch and the switching time. The switching time (lower curve) depends primarily on parameter LuxR. Switching time ranges from zero for high LuxR values (i.e., approaching the static strategy, where the manipulated genes are turned off immediately) to the total batch time for small LuxR values (thus resulting in the other extreme, cells operating in the ON state throughout the batch). Similar features are observed in the two extreme operating points for yield and titer (Figure 6B and C). The process approaches the static strategy for high LuxR values and as a result yield and titer converge to their maximum values.

Effect of γ_C and LuxR. In Figure 7A, the productivity of the dynamic strategy is again higher than the static in most of the γ_C-LuxR parameter space and the maximum productivity converges to the value of the ideal ON-OFF controller (3 mM serine/h). The plateau is narrow, similarly to the α_C-LuxR space, however in this case both γ_C and LuxR seem to affect the productivity (in contrast to the previous pair of parameters where LuxR mostly affected productivity). Productivity is favored by either high LuxR–low γ_C, or low LuxR–high γ_C values.

The effect of parameters γ_C and LuxR on the batch and the switching time is elucidated in Figure 7D (notice that the axes direction is reversed). Here, both γ_C and LuxR affect the switching time, in contrast with the previous pair of parameters where α_C did not affect the switching time. This implies that the interaction between parameters γ_C and LuxR is strong. High values of γ_C and LuxR lead to an instantaneous switch, and the values of the objectives tend toward the static strategy values. At the other extreme, gene expression remains in the ON state throughout the batch for low values of γ_C and LuxR, resulting in wild-type cells and minimum objective values.

Summary of the Effects of Changing Two Parameters at a Time. Considering the objective surfaces in Figure 5, values of α_C and γ_C must be chosen to ensure that the productivity lies in the optimal plateau region. To achieve balanced productivity and yield, high γ_C and low α_C over the plateau are desired (i.e., values that correspond to the left side of the plateau shown in Figure 5A). High α_C values increase the optimal plateau area. However, very strong promoters could lead to low growth rate due to increased metabolic burden associated with the genetic circuit and should be avoided.

The analysis also suggests that LuxR concentration can be manipulated to fine-tune the switching time (Figure 6). The engineering of LuxR promoters and design of synthetic ribosome binding sites (RBS) can be used to modify the value of LuxR concentration.[24,34] We also showed that parameter LuxR strongly interacts with γ_C (Figure 7) and that they both affect the switching time. Therefore, switching time is sensitive with respect to parameters LuxR and γ_C.

Up to this point, we have identified the three most influential parameters, the interactions between them in a pairwise manner, and how they affect the key features of the dynamic strategy, namely, the bistability of the toggle and the switching time. Parameters α_C and γ_C affect the bistability of the toggle switch, and the design of the integrated circuit must guarantee that the circuit is bistable. Parameters γ_C and LuxR strongly influence the switching time in a synergistic way, and therefore fine-tuning of the switching time is possible. In the next section, the objective of the analysis is to determine the final parameter region that satisfies the yield and productivity targets.

Effect of All Three Parameters. To visualize the effect of all three parameters when varied at the same time, we generated the isosurface plots of productivity and yield with respect to parameters α_C, γ_C, and LuxR (Supplementary Figures SI.3 and SI.4, respectively). The volume of the isosurface shows the solution space that satisfies targets, and it increases as we relax the target values. Supplementary Figure SI.3 shows that high α_C and γ_C values are increasing the solution space of the strategy as indicated by the increased volume of the plot in the high α_C and γ_C region (in agreement with Figure 5). Second, the shape of the volume demonstrates the outcome of Figure 7 that either high LuxR–low γ_C or low LuxR–high γ_C values are

dx.doi.org/10.1021/sb300129j | ACS Synth. Biol. 2013, 2, 442–452

optimal for productivity. The same result is observed in Supplementary Figure SI.3, where we can isolate two subvolumes of maximum productivity: one for high LuxR and low γ_C and one for low LuxR and high γ_C values. Considering the effect of the parameters on the yield of the process (Supplementary Figure SI.4) allows us to prune the optimal parameter space. The maximum yield volume is located at the tip of the parameter cube, for low α_C and high γ_C and LuxR values, which leans toward the static strategy.

In Figure 8, we overlap the two volumes for decreasing levels of productivity and yield to identify regions in the parameter space where the target values indicated are satisfied. In Figure 8A, the targets for productivity and yield are very high (i.e., 2.9 mM serine/h and 1.2 mM serine/mM glucose, respectively), and the volume in the parameter space to achieve these thresholds is a thin horizontal slice that lies between values of LuxR of 0.5 and 1.5 μM. The shape of the volume indicates that in order to achieve the highest values for productivity and yield, fine-tuning of LuxR concentration is crucial.

Next, the target for productivity is relaxed to 2.8 mM serine/h (Figure 8B). The volume lies between LuxR values of 0.5 and 2.5 μM in most of the parameter space, which supports the outcome of Figure 8A that tight regulation of LuxR between 0.5 and 1.5 μM can lead to the highest values of productivity and yield. Another interesting feature here is the growth of a subvolume toward higher LuxR values for low γ_C. This is also observed when the yield target is reduced to 1.1 mM serine/mM glucose (Figure 8C) and when both productivity and yield are reduced to 2.8 mM serine/h and 1.1 mM serine/mM glucose, respectively (Figure 8D). The subvolume for low γ_C and LuxR > 2 values is less robust than the horizontal subvolume, since it requires tight fine-tuning of both α_C (0.4 to 10 μM/min) and γ_C (1−2/min). This implies that operating in this subvolume could potentially cause loss of the bistability if α_C and γ_C are not tuned precisely. Therefore, it is recommended that the operating volume be chosen as the volume shown in Figure 8A.

Preliminary Design Considerations. The sensitivity-based model analysis presented here has given us insight into the design and optimization of the dynamic control strategy. The results of the global sensitivity analysis were used to reduce the model complexity by identifying a set of key parameters (i.e., α_C, γ_C, and LuxR) that have the greatest effect on serine production. Furthermore, we have identified the ranges of the key parameters that satisfy productivity and yield targets. In order to design a stable and robust system that balances productivity and yield, we need to identify an optimal operating region. Considering the uncertainties associated with parameter estimation and noise in gene expression, we believe that proposing an operating region is more appropriate than suggesting a single set of parameter values.

The key parameters can be adjusted using standard molecular biology techniques. To this end, the protein synthesis rate constant α_C and the LuxR protein concentration can be manipulated by designing synthetic ribosome binding sites.[24] Manipulating LuxR concentration can be challenging, as the protein degrades in the absence of AHL (reported half-time of 65 min[58]). The fast growth in the first phase will lead to AHL production and formation of the slow-degrading LuxR-AHL complex, which accumulates at high concentration.[59] The protein decay constant γ_C can be engineered either by using degradation tags to reduce the half-life of the proteins[60] or by using temperature-sensitive mutants of the LacI.[61]

To summarize the effect of the main parameters, α_C and γ_C have their greatest effect on the bistability of the genetic circuit. This result is in agreement with previously published model analysis and experimental validation by Gardner et al. for the toggle switch alone. The interaction between α_C and γ_C does not influence the switching time significantly. LuxR concentration has a major impact on both the bistability of the switch and the switching time. Specifically, when interacting with parameter γ_C, the switching time depends strongly on both LuxR and γ_C. In the last part of the analysis, changing all three parameters simultaneously revealed that it if we use values of γ_C and α_C to ensure bistability of the switch, we can use LuxR to manipulate the switching time of the circuit in order to achieve high productivity and yield targets close to the maximum theoretical values.

A final recommended range for LuxR is between 0.5 and 1.5 μM, with preference for values close to 1.5 to achieve higher yield. To visualize the optimal parameter design space of α_C and γ_C, the top view of Figure 8A is shown in Figure 9. Parameter γ_C

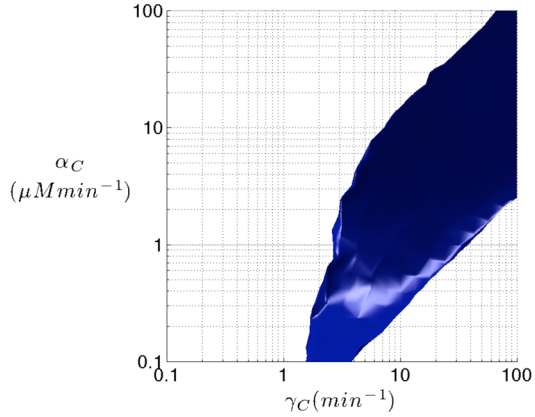

Figure 9. Optimal parameter design space of α_C and γ_C to achieve productivity higher than 2.9 mM serine/h and yield higher than 1.2 mM serine/mM glucose. This figure is the top view of Figure 8A. Values of LuxR of this volume are between 0.5 and 1.5 μM.

must be at least 1.5/min to achieve the target yield and productivity values. For increasing values of γ_C, the range of α_C also increases. Due to stochastic effects arising from transcription and translation noise, individual cells will have slightly different boundaries than Figure 9, and as a consequence operating close to the boundaries will likely lead to lower objective values. It has been previously shown that the toggle switch is resistant to noise-induced transitions, and this is due to the high transcription rates.[37] Low transcription rates (i.e., α_C) can result in spontaneous switching between the states.[62,63] Hence, the recommended operating region is in the middle of the optimal design space shown in Figure 9 aiming toward higher values of α_C and γ_C where the width of the optimal design space increases. Nevertheless, very high values of both parameters should be avoided because of the metabolic burden associated with high expression (high values of α_C and γ_C mean high production rate and high degradation rate of proteins). These results now set the stage for the experimental implementation of the dynamic control strategy.

Conclusions. We have performed both analysis and design of our integrated model of a genetic circuit coupled to bacterial metabolism for the production of serine. By manipulating the switching time of the ideal ON-OFF control, we showed that

the maximum theoretical productivity of the dynamic strategy is 29.6% higher than the static strategy, for an optimal switching time of approximately 4 h. The initial design of the genetic circuit was applied using parameter values from the literature and it showed a 28.3% increase in productivity compared to the static strategy, very close to the maximum theoretical productivity. In order to explore the sensitivity of serine concentration to the parameters of the genetic circuit, we applied global sensitivity analysis (GSA) to identify the parameters with the highest impact on serine concentration. GSA identified three key parameters (i.e., α_C, γ_C, and LuxR), thus reducing model complexity and allowing for further simulations to investigate the relationship between these parameters and the bioengineering objectives. In turn, these results have enabled us to identify the optimal parameter design space required to operate the genetic circuit at both high productivity and yield, setting the stage for experimental implementation.

METHODS

Dynamic Flux Balance Analysis. Metabolism of *E. coli* was modeled using the dynamic Flux Balance Analysis (dFBA) framework.[12] The dynamics of the quorum sensing and the toggle switch are modeled using mechanistic equations.[31,32] The coupling of bacterial metabolism to the genetic circuit is captured in the third constraint of the FBA, with the manipulated fluxes v_C being proportional to the C concentration (eq 4). A schematic description of the genetic circuit is shown in Figure 1. The model is reproduced here for completeness. In this model, AHL is assumed to diffuse freely and its intracellular and extracellular concentrations are assumed to be equal.[64] For a detailed description refer to Anesiadis et al.[36,57]

$$\text{maximize } v^{\text{growth}}(t_i) \tag{1}$$

$$\text{subject to: } \sum_{j=1}^{M} S_{kj} v_j(t_i) = 0 \text{ for } k = 1, ..., M \tag{2}$$

$$v_{\min} \le v_j(t_i) \le v_{\max} \text{ for } j = 1, ..., N \tag{3}$$

$$v_{cj}(t_i) = \gamma_{cj} \cdot C(t_i) \text{ for } cj = 1, ..., U \tag{4}$$

$$\frac{dX}{dt} = v^{\text{growth}}(t_i) \cdot X \tag{5}$$

$$\frac{dP}{dt} = v^{\text{product}}(t_i) \cdot X \tag{6}$$

$$\frac{dA}{dt} = v_A X - \gamma_A A \tag{7}$$

$$\frac{dR}{dt} = \rho_R [\text{LuxR}]^2 A^2 - \gamma_R R \tag{8}$$

$$\frac{dL}{dt} = \frac{a_{L1}}{1 + \left(\frac{C}{\beta_C}\right)^2} + \frac{a_{L2} R^3}{\theta_R + R^3} - \gamma_L L \tag{9}$$

$$\frac{dC}{dt} = \frac{a_C}{1 + \left(\frac{L}{\beta_L}\right)^2} - \gamma_C C \tag{10}$$

$$t_i = t_0 + i \cdot T_s, \text{ for } i = 0, ..., f$$

The dFBA parameters include S, the stoichiometric matrix of the reactions; v_j, the flux j; v^{product}, the vector of product fluxes; v^{growth}, the growth rate; and $v_{\min}$ and $v_{\max}$, the vectors of lower and upper limits of the fluxes. The total number of metabolites is M, the total number of fluxes is N, and the total number of manipulated fluxes is U. Also, X is the biomass concentration, and P is the product concentration. The genetic circuit variables A, R, L, and C are the AHL, LuxR-AHL complex, LacI, and λCI concentration, respectively. Parameter v_A is the AHL production rate constant, α_{L1}, α_{L2}, α_C are the protein LacI and λCI synthesis rate constants, β_L and β_C are the LacI and λCI repression coefficients, γ_A, γ_R, γ_L, and γ_C are the AHL, complex, LacI, and λCI protein decay constants, θ_R is the complex activation coefficient, ρ_R is the complex dimerization constant, and [LuxR] is the protein LuxR concentration. Finally, the batch time $(t_0 - t_f)$ is divided into f intervals of length T_s equal to 0.05 h.

Although the majority of the quorum sensing systems shows no cooperativity (e.g., the LuxR−AHL complex has a Hill coefficient of 1), we used a Hill coefficient of 3 in eq 9. This was done to achieve sharper dynamics, similar to the dynamics reported by Gardner et al. Highly cooperative protein−DNA interactions have been reported in the quorum sensing regulator CepR of *Burkholderia cenocepacia*, and therefore a Hill coefficient of 3 is realistic in an experimental context.[65]

The latest genome-scale model of *E. coli* metabolism, *i*JO1366, was used in all simulations.[66] The stoichiometry matrix S of the model includes 2583 reactions and 1805 metabolites. The maximum glucose and oxygen uptake rate used in the simulations is 10 and 20 mmol/gDW/h, respectively. These values are typically used in FBA simulations.[66] The integration was performed using the ode23s MATLAB solver (The Mathworks, Inc., Natick, MA) over 12 h to ensure full consumption of the glucose for the slowest growing case which is the knockout static strategy. The LP problem was solved in MATLAB, using CPLEX 11.2 with the CPLEXINT MATLAB interface. All simulations were run on a Red Hat Enterprise Linux Server 5.8 with 8 hexa-core AMD Opteron processors and 256 GB of RAM.

Global Sensitivity Analysis. Here we used the Sobol' global sensitivity method for parameter ranking.[67,47] This is a variance-based Monte Carlo method that explores the parameter space by changing all parameters simultaneously, as opposed to local methods, and generates estimates of the first-order, interaction and total sensitivities indices. Parameters with a total sensitivity index less than 0.1 have negligible effect on the output and can be fixed at their nominal values, whereas parameters with higher indices have a significant impact on the output.

Following Saltelli's implementation, two random matrices of the parameter space A and B are generated using MATLAB routine sobolset.[47] Matrices A and B are $K \times n$ dimensions, where K is the sample size and n is the number of the parameters varied. From matrix B, n matrices C_i $(i = 1, ..., n)$ are generated with all columns of B except the i-th, which is taken from matrix A. Then the model is evaluated for all the parameter sets in matrices A, B, and C_i (i.e., $K \cdot (n + 2)$ times) and the outputs of interest y_A, y_B, and y_{Ci} (i.e., serine concentration) are used to calculate the first-order or individual S_i^{ind} and total sensitivity estimates S_i^{T} based on the following equations:

dx.doi.org/10.1021/sb300129j | ACS Synth. Biol. 2013, 2, 442−452

$$S_i^{\text{ind}} = \frac{y_A \cdot y_{Ci} - \frac{1}{K} \cdot \sum_{j=1}^{K} y_A^j \cdot y_B^j}{y_A \cdot y_A - \left(\frac{1}{K} \cdot \sum_{j=1}^{K} y_A^j\right)^2} \quad (11)$$

$$S_i^{\text{T}} = 1 - \frac{y_B \cdot y_{Ci} - \left(\frac{1}{K} \cdot \sum_{j=1}^{K} y_A^j\right)^2}{y_B \cdot y_B - \left(\frac{1}{K} \cdot \sum_{j=1}^{K} y_B^j\right)^2} \quad (12)$$

The interaction indices, S_i^{int} are then calculated as the difference between the total and the individual indices: $S_i^{\text{int}} = S_i^{\text{T}} - S_i^{\text{ind}}$.

In our model, all parameters of the genetic circuit ($n = 13$) were varied between 0.1× and 10× of their nominal values. Convergence of the GSA estimates was achieved when the number of model evaluations was greater than 8000, therefore $K = 8000$ was used for the results presented here. The total number of model evaluations in Saltelli's implementation is $K \cdot (n + 2) = 120{,}000$. The model evaluation step was anticipated to be the most time-consuming, and therefore we parallelized the model evaluation over 15 different processors (i.e., $n + 2$) and the results were obtained within 2 days.

Analysis of the Most Sensitive Parameters. Once we identified that there were three parameters with total sensitivity indices higher than 0.1, we evaluated the effect of these parameters on important variables of the bioprocess such as productivity, yield, titer, batch, and switching time. Productivity and yield were calculated at the end of the batch using the following equations:

$$\text{productivity} = \frac{\text{serine produced}}{\text{batch time}} = \frac{\text{mM serine}}{\text{h}} \quad (13)$$

$$\text{yield} = \frac{\text{serine produced}}{\text{glucose consumed}} = \frac{\text{mM serine}}{\text{mM glucose}} \quad (14)$$

Batch time was estimated as the time at which glucose was fully consumed and switching time as the time at which the manipulated fluxes reached 5% of their initial values.

To visualize the results, we separately varied two (three possible pairs) and three parameters at a time over a 25-point grid in each dimension and plotted the five variables of interest, while keeping all other parameters of the genetic circuit at their nominal values. Here, we varied the parameters over a range wider than the sensitivity analysis in order to examine all possible behaviors and parameter regions.

■ ASSOCIATED CONTENT

Supporting Information

Supporting figures and tables. This material is available free of charge via the Internet at http://pubs.acs.org.

■ AUTHOR INFORMATION

Corresponding Author

*Tel: +1 416 946 0996. Fax: +1 416 978 8605. E-mail: krishna.mahadevan@mail.utoronto.ca.

Author Contributions

All authors contributed to the design of the research and the writing of the paper. N.A. performed the simulations.

Notes

The authors declare no competing financial interest.

■ ACKNOWLEDGMENTS

The authors thank Laurence Yang for the implementation of the EMILiO algorithm and Christina Heidorn for the preparation of Figure 1.

■ REFERENCES

(1) Keasling, J. (2010) Manufacturing molecules through metabolic engineering. *Science 330*, 1355−1358.

(2) Yadav, V. G., DeMey, M., Lim, C. G., Ajikumar, P. K., and Stephanopoulos, G. (2012) The future of metabolic engineering and synthetic biology: Towards a systematic practice. *Metab. Eng. 14*, 233−241.

(3) Oberhardt, M., Palsson, B. O., and Papin, J. A. (2009) Applications of genome-scale metabolic reconstructions. *Mol. Syst. Biol. 5*, 320.

(4) Copeland, W. B., Bartley, B. A., Chandran, D., Galdzicki, M., Kim, K. H., Sleight, S. C., Maranas, C. D., and Sauro, H. M. (2012) Computational tools for metabolic engineering. *Metab. Eng. 14*, 270−280.

(5) Burgard, A. P., Pharkya, P., and Maranas, C. D. (2003) OptKnock: a bilevel programming framework for identifying gene knockout strategies for microbial strain optimization. *Biotechnol. Bioeng. 84*, 647−657.

(6) Pharkya, P., and Maranas, C. D. (2006) An optimization framework for identifying reaction activation/inhibition or elimination candidates for overproduction in microbial systems. *Metab. Eng. 8*, 1−13.

(7) Lun, D. S., Rockwell, G., Guido, N. J., Baym, M., Kelner, J. A., Berger, B., Galagan, J. E., and Church, G. M. (2009) Large-scale identification of genetic design strategies using local search. *Mol. Syst. Biol. 5*, 296.

(8) Ranganathan, S., Suthers, P. F., and Maranas, C. D. (2010) OptForce: an optimization procedure for identifying all genetic manipulations leading to targeted overproductions. *PLoS Comput. Biol. 6* (4), e1000744.

(9) Yang, L., Cluett, W. R., and Mahadevan, R. (2011) EMILiO: a fast algorithm for genome-scale strain design. *Metab. Eng. 13*, 272−281.

(10) Banga, J. R., Balsa-Canto, E., Moles, C. G., and Alonso, A. A. (2003) Dynamic optimization of bioreactors: a review. *Proc. Indian Natl. Sci. Acad. 69A*, 257−265.

(11) Varma, A., and Palsson, B. O. (1994) Stoichiometric flux balance models quantitatively predict growth and metabolic by-product secretion in wild-type *Escherichia coli* W3110. *Appl. Environ. Microbiol. 60*, 3724−3731.

(12) Mahadevan, R., Edwards, J. S., and Doyle, F. J., III (2002) Dynamic flux balance analysis of diauxic growth in *Escherichia coli*. *Biophys. J. 83*, 1331−1340.

(13) Hjersted, J. L., and Henson, M. A. (2006) Optimization of fed-batch *Saccharomyces cerevisiae* fermentation using dynamic flux balance models. *Biotechnol. Prog. 22*, 1239−1248.

(14) Gadkar, K. G., Doyle, F. J., III, Edwards, J. S., and Mahadevan, R. (2005) Estimating optimal profiles of genetic alterations using constraint-based models. *Biotechnol. Bioeng. 89*, 243−251.

(15) Gadkar, K. G., Mahadevan, R., and Doyle, F. J., III (2006) Optimal genetic manipulations in batch bioreactor control. *Automatica 42*, 1723−1733.

(16) San, K. Y., and Stephanopoulos, G. (1984) A note on the optimality criteria for maximum biomass production in a fed-batch fermentor. *Biotechnol. Bioeng. 26* (10), 1261−1264.

(17) Purnick, P. E. M., and Weiss, R. (2009) The second wave of synthetic biology: from modules to systems. *Nat. Rev. Mol. Cell Biol. 10*, 410−422.

(18) Khalil, A. S., and Collins, J. J. (2010) Synthetic biology: applications come of age. *Nat. Rev. Genet. 11*, 367−379.

(19) Nandagopal, N., and Elowitz, M. B. (2011) Synthetic biology: integrated gene circuits. *Science 333*, 1244−1248.

(20) Voigt, C. A. (2006) Genetic parts to program bacteria. *Curr. Opin. Biotechnol. 17*, 548−557.
(21) Alper, H., Fischer, C., Nevoigt, E., and Stephanopoulos, G. (2005) Tuning genetic control through promoter engineering. *Proc. Natl. Acad. Sci. U.S.A. 102*, 12678−12683.
(22) Alper, H., and Stephanopoulos, G. (2007) Global transcription machinery engineering: a new approach for improving cellular phenotype. *Metab. Eng. 9*, 258−267.
(23) Ellis, T., Wang, X., and Collins, J. J. (2009) Diversity-based, model-guided construction of synthetic gene networks with predicted functions. *Nat. Biotechnol. 27*, 465−471.
(24) Salis, H. M., Mirsky, E. A., and Voigt, C. A. (2009) Automated design of synthetic ribosome binding sites to control protein expression. *Nat. Biotechnol. 27*, 946−950.
(25) Culler, S. J., Hoff, K. G., and Smolke, C. D. (2010) Reprogramming cellular behaviour with RNA controllers responsive to endogenous proteins. *Science 330*, 1251−1255.
(26) Carothers, J. M., Goler, J. A., Juminaga, D., and Keasling, J. D. (2011) Model-driven engineering of RNA devices to quantitatively program gene expression. *Science 334*, 1716−1719.
(27) Boyle, P. M., and Silver, P. A. (2012) Part plus pipes: synthetic biology approaches to metabolic engineering. *Metab. Eng. 14*, 223−232.
(28) Callura, J. M., Cantor, C. R., and Collins, J. J. (2012) Genetic switchboard for synthetic biology applications. *Proc. Natl. Acad. Sci. U.S.A. 109*, 5850−5855.
(29) Keasling, J. (2012) Synthetic biology and the development of tools for metabolic engineering. *Metab. Eng. 14*, 189−195.
(30) Kobayashi, H., Kaern, M., Araki, M., Chung, K., Gardner, T. S., Cantor, C. R., and Collins, J. J. (2004) Programmable cells: interfacing natural and engineered gene networks. *Proc. Natl. Acad. Sci. U.S.A. 101*, 8414−8419.
(31) You, L., Cox, R. S., III, Weiss, R., and Arnold, F. H. (2004) Programmed population control by cell-cell communication and regulated killing. *Nature 428*, 868−871.
(32) Basu, S., Gerchman, Y., Collins, C. H., Arnold, F. H., and Weiss, R. (2005) A synthetic multicellular system for programmed pattern formation. *Nature 434*, 1130−1134.
(33) Tsao, C., Hooshangi, S., Wu, H. C., Valdes, J. J., and Bentley, W. E. (2010) Autonomous induction of recombinant proteins by minimally rewiring native quorum sensing regulon of *E. coli*. *Metab. Eng. 12*, 291−297.
(34) Collins, C. H., Arnold, F. H., and Leadbetter, J. R. (2005) Directed evolution of *Vibrio fischeri* LuxR for increased sensitivity to a broad spectrum of acyl-homoserine lactones. *Mol. Microbiol. 55*, 712−723.
(35) Collins, C. H., Leadbetter, J. R., and Arnold, F. H. (2006) Dual selection enhances the signaling specificity of a variant of the quorum-sensing transcriptional activator LuxR. *Nat. Biotechnol. 24*, 708−712.
(36) Anesiadis, N., Cluett, W. R., and Mahadevan, R. (2008) Dynamic metabolic engineering for increasing bioprocess productivity. *Metab. Eng. 10*, 255−266.
(37) Gardner, T. S., Cantor, C. R., and Collins, J. J. (2000) Construction of a genetic toggle switch in *Escherichia coli*. *Nature 403*, 339−342.
(38) Van Riel, N. A. W. (2006) Dynamic modeling and analysis of biochemical networks: mechanism-based models and model-based experiments. *Briefings Bioinf. 7*, 364−374.
(39) Haseltine, E. L., and Arnold, F. H. (2007) Synthetic gene circuits: design with directed evolution. *Annu. Rev. Biophys. Biomol. Struct. 36*, 1−19.
(40) Chandran, D., Copeland, W. B., Sleight, S. C., and Sauro, H. M. (2008) Mathematical modeling and synthetic biology. *Drug Discovery Today: Dis. Models 5*, 299−309.
(41) Zheng, Y., and Sriram, G. (2010) Mathematical modelling: bridging the gap between concept and realization in synthetic biology. *J. Biomed. Biotechnol.*, DOI: 10.1155/2010/541609.
(42) Biliouris, K., Daoutidis, P., and Kaznessis, Y. N. (2011) Stochastic simulations of the tetracycline operon. *BMC Syst. Biol. 5*, 9.
(43) Saltelli, A., Ratto, M., Andres, T., Campolongo, F., Cariboni, J., Gatelli, D., Saisana, M., and Tarantola, S. (2008) *Global Sensitivity Analysis: The Primer*, Wiley, New York.
(44) Kiparissides, A., Kucherenko, S. S., Mantalaris, A., and Pistikopoulos, E. N. (2009) Global sensitivity analysis challenges in biological systems modelling. *Ind. Eng. Chem. Res. 48*, 7168−7180.
(45) Kiparissides, A., Koutinas, M., Kontoravdi, C., Mantalaris, A., and Pistikopoulos, E. N. (2011) 'Closing the loop' in biological systems modeling - From the *in silico* to the *in vitro*. *Automatica 47*, 1147−1155.
(46) Miskovic, L., and Hatzimanikatis, V. (2011) Modeling of uncertainties in biochemical reactions. *Biotechnol. Bioeng. 108*, 413−423.
(47) Saltelli, A. (2002) Making best use of model evaluations to compute sensitivity indices. *Comput. Phys. Commun. 145*, 280−297.
(48) Feng, X., Hooshangi, S., Chen, D., Li, G., Weiss, R., and Rabitz, H. (2004) Optimizing genetic circuits by global sensitivity analysis. *Biophys. J. 87*, 2195−2202.
(49) Miller, G. M., Ogunnaike, B. A., Schwaber, J. S., and Vadigepalli, R. (2010) Robust dynamic balance of AP-1 transcription factors in a neuronal gene regulatory network. *BMC Syst. Biol. 4*, 171.
(50) Zheng, Y., and Rundell, A. (2006) Comparative study of parameter sensitivity analyses of the TCR-activated Erk-MAPK signalling pathway. *IEE Proc. Syst. Biol. 153*, 201−211.
(51) Chu, Y., Jayaraman, A., and Hahn, J. (2007) Parameter sensitivity analysis of IL-6 signalling pathways. *IET Syst. Biol. 1*, 342−352.
(52) Zhao, J., Fang, Y., Scheibe, T. D., Lovley, D. R., and Mahadevan, R. (2010) Modeling and sensitivity analysis of electron capacitance for Geobacter in sedimentary environments. *J. Contam. Hydrol. 112*, 30−44.
(53) Zhao, J., Scheibe, T. D., and Mahadevan, R. (2011) Model-based analysis of the role of biological, hydrological and geochemical factors affecting uranium bioremediation. *Biotechnol. Bioeng. 108*, 1537−1548.
(54) Kiparissides, A., Koutinas, M., Moss, T., Newman, J., Pistikopoulos, E. N., and Mantalaris, A. (2011) Modelling the Delta1/Notch1 pathway: in search of the mediator(s) of neural stem cell differentiation. *PLoS One 6* (2), e14668.
(55) Kontoravdi, C., Asprey, S. P., Pistikopoulos, E. N., and Mantalaris, A. (2005) Application of global sensitivity analysis to determine goals for design of experiments: an example study on antibody-producing cell cultures. *Biotechnol. Prog. 21*, 1128−1135.
(56) Ho, Y., Kiparissides, A., Pistikopoulos, E. N., and Mantalaris, A. (2012) Computational approach for understanding and improving GS-NSO antibody production under hyperosmotic conditions. *J. Biosci. Bioeng. 113*, 88−98.
(57) Anesiadis, N., Cluett, W. R., Mahadevan, R. (2011) Model-driven design based on sensitivity analysis for a synthetic biology application. In *Proceedings of the 21st European Symposium on Computer-Aided Process Engineering-ESCAPE 21* (Pistikopoulos, E. N., Georgiadis, M. C., Kokossis, A. C., Eds.), Vol. *29*, pp 1446−1450, Elsevier, Amsterdam.
(58) Manefield, M., Rasmussen, T. B., Henzter, M., Andersen, J. B., Steinberg, P., Kjelleberg, S., and Givskov, M. (2002) Halogenated furanones inhibit quorum sensing through accelerated LuxR turnover. *Microbiology 148*, 1119−1127.
(59) Huang, D., Holtz, W. J., and Maharbiz, M. M. (2012) A genetic bistable switch utilizing nonlinear protein degradation. *J. Biol. Eng. 6*, 9.
(60) Fung, E., Wong, W. W., Suen, J. K., Bulter, T., Lee, S., and Liao, J. C. (2005) A synthetic gene-metabolic oscillator. *Nature 435*, 118−122.
(61) McCabe, K. M., Lacherndo, E. J., Albino-Flores, I., Sheehan, E., and Hernandez, M. (2011) LacI(Ts)-regulated expression as an in situ intracellular biomolecular thermometer. *Appl. Environ. Microbiol. 77* (9), 2863−2868.
(62) Elowitz, M. B., Levine, A. J., Siggia, E. D., and Swain, P. S. (2002) Stochastic gene expression in a single cell. *Science 297*, 1183−1186.

(63) Isaacs, F. J., Hasty, J., Cantor, C. R., and Collins, J. J. (2003) Prediction and measurement of an autoregulatory genetic module. *Proc. Natl. Acad. Sci. U.S.A. 100*, 7714−7719.
(64) Kaplan, H. B., and Greenberg, E. P. (1985) Diffusion of autoinducer is involved in regulation of the *Vibrio fischeri* luminescence system. *J. Bacteriol. 163*, 1210−1214.
(65) Weingart, C. L., White, C. E., Liu, S., Chai, Y., Cho, H., Tsai, C.-S., Wei, Y., Delay, N. R., Gronquist, M. R., Eberhard, A., and Winans, S. C. (2005) Direct binding of the quorum sensing regulator CepR of *Burkholderia cenocepacia* to two target promoters in vitro. *Mol. Microbiol. 57*, 452−467.
(66) Orth, J. D., Conrad, T. M., Na, J., Lerman, J. A., Nam, H., Feist, A. M., and Palsson, B. O. (2011) A comprehensive genome-scale reconstruction of *Escherichia coli* metabolism. *Mol. Syst. Biol. 7*, 535.
(67) Sobol, I. M. (2001) Global sensitivity indices for nonlinear mathematical models and their Monte Carlo estimates. *Math. Comput. Simul. 55*, 271−280.